Aerosol and Air Quality Research, 16: 555–567, 2016

ISSN: 1680-8584 print / 2071-1409 online
doi: 10.4209/aaqr.2015.05.0346

Transported Mineral Dust Deposition Case Study at a Hydrologically Sensitive Mountain Site: Size and Composition Shifts in Ambient Aerosol and Snowpack

Jessica L. Axson[1], Hongru Shen[1], Amy L. Bondy[2], Christopher C. Landry[3], Jason Welz[3], Jessie M. Creamean[4,5*], Andrew P. Ault[1,2*]

[1] *Department of Environmental Health Sciences, University of Michigan, Ann Arbor, MI, USA*
[2] *Department of Chemistry, University of Michigan, Ann Arbor, MI, USA*
[3] *Center for Snow & Avalanche Studies, Silverton, CO, USA*
[4] *Cooperative Institute for Research in Environmental Sciences, University of Colorado, Boulder, CO, USA*
[5] *Physical Sciences Division, NOAA Earth System Research Laboratory, Boulder, CO, USA*

ABSTRACT

Transported mineral dust deposition to remote mountain snow decreases snow albedo and increases absorption of solar radiation, which accelerates snowpack melt and alters water supply. Mineralogy and chemical composition determine dust particle optical properties, which vary by source region. While impacts of dust deposition at remote mountain sites have been established, few studies have connected the chemical composition of ambient particles during deposition events with the properties of those deposited on the snowpack. Ambient particles and surface snow were sampled in the San Juan Mountains of southwestern Colorado, which frequently experiences dust deposition in the spring and has evidence of dust-enhanced snow melt. Individual particles were analyzed using scanning electron microscopy with energy dispersive X-ray spectroscopy (SEM-EDX). The number concentration and size distribution of insoluble residues in the top level of snow were determined with nanoparticle tracking analysis (NTA). During a minor dust event (April 2–3, 2015), the fraction of absorbing iron-enriched dust in the ambient aerosol, the number concentration, and size of insoluble residues in snow all increased. This can be traced to shifts in mineral dust source region within the Colorado Plateau, during which, there were higher wind speeds leading to increased transport. The shift in chemical composition and mineralogy of the transported dust has the potential to impact snowpack radiative forcing during dry deposition. In addition, it can also modify the snowpack through scavenging of particles during wet deposition, as well as alter the properties of clouds and orographic precipitation. Understanding these impacts is crucial to understanding the hydrological cycle at remote mountain sites.

Keywords: Mineral dust; Atmospheric aerosols; Atmospheric chemistry; Climate change; Long-range transport; Radiative effects.

INTRODUCTION

It is well known that mineral dust deposition onto mountain snowpack decreases snow albedo and modifies regional hydrological cycles (Warren and Wiscombe, 1980; Conway *et al.*, 1996; Painter *et al.*, 2007; Lau *et al.*, 2010; Painter *et al.*, 2012). The effect of dust deposition on snowpack and the hydrological cycle has been monitored for several years in the Senator Beck Basin Study Area (SBBSA), a remote mountain region in the San Juan Mountains of southwest Colorado (Painter *et al.*, 2007; Lawrence *et al.*, 2010; Painter *et al.*, 2012). Previous studies have determined that dust deposited in the San Juan Mountains primarily originates from the southwestern United States, particularly the southern portion of the Colorado Plateau, which encompasses the northern sections of Arizona and New Mexico, southeast Utah and southwest Colorado (Painter *et al.*, 2007; Neff *et al.*, 2008; Lawrence *et al.*, 2010; Painter *et al.*, 2012). These dust events decrease snow albedo and lead to increases in surface absorption by mineral dust in the visible region, where the solar radiation spectrum peaks, and increases in snow grain growth, enhancing absorption in the near infrared (Warren and Wiscombe, 1980; Conway *et al.*, 1996; Sokolik and Toon, 1996; Lafon *et al.*, 2006; Painter *et al.*, 2007). This is especially important as the intensity of solar radiation increases in the spring. As the mineral dust absorbs radiation, the snowpack warms and melts, causing an earlier annual decrease in snowpack by 21–51 days (Skiles *et al.*, 2012) and subsequent earlier release of snow melt water. Additional

* Corresponding author.
Tel.: (734)-763-4212; (303)-497-4432; Fax: (734) 936-7283
E-mail addresses: aulta@umich.edu, jessie.creamean@noaa.gov

important contributions to snow albedo and melt observed in other regions is the deposition of black carbon, which also strongly absorbs solar radiation (Bond *et al.*, 2013), however its contribution to radiative forcing has not yet been quantified in this location. The timing and volume of snow melt water is important in determining water resources, as this region provides a water source for much of the southwestern United States (Painter *et al.*, 2007; Skiles *et al.*, 2012; Deems *et al.*, 2013). Changes in mineral dust deposition and radiative forcing, therefore, are very important to understanding the amount and timing of freshwater provided by the snow melt.

A key issue in determining the radiative forcing of the transported and deposited dust is the chemical composition, particularly the mineralogy, and whether there is a difference in composition during deposition events. This is important as changes in source region will alter the mineralogy of the dust deposited during events (Painter *et al.*, 2007; Lawrence *et al.*, 2010; Di Biagio *et al.*, 2014). The optical properties of mineral dust varies dramatically between minerals, specifically, the absorption terms (k, the imaginary term) in their complex refractive indices, which can range from 1.5 (typical of quartz and calcite) up to about 3.2 (typical of hematite) (Sokolik and Toon, 1999). For instance, iron (Fe) rich minerals and clays absorb short wave (visible and ultraviolet) radiation, whereas quartz and calcium (Ca) rich minerals absorb more long wave (infrared) radiation (Sokolik and Toon, 1999; Hudson *et al.*, 2008a; Hudson *et al.*, 2008b; Kleiber *et al.*, 2009; Klueser *et al.*, 2012; Laskina *et al.*, 2012). Individual particles in the atmosphere are often mixtures of multiple minerals (Ault *et al.*, 2012; Sobanska *et al.*, 2012; Jung *et al.*, 2014; Sobanska *et al.*, 2014), which complicates understanding their specific optical properties. Determining the relative amounts of these minerals in the dust will allow for a more accurate calculation of their optical properties and ultimate effect on snow melt.

Although dust deposition has been extensively studied in the snowpack for the San Juan Mountains, to date the properties of the transported, ambient mineral dust aerosol have not been thoroughly investigated or linked with the properties of the mineral dust present in the snow. Atmospheric mineral dust affects global radiative forcing directly by absorbing and scattering solar radiation and indirectly through altering cloud properties (DeMott *et al.*, 2003a, b; Andreae and Rosenfeld, 2008; Ault *et al.*, 2011; Baustian *et al.*, 2012; Creamean *et al.*, 2013). Mineral dust aerosol direct absorption effects are, like that deposited on snow, strongly dependent on the mineral composition with Fe containing dust showing strong absorption in the atmosphere (Sokolik and Toon, 1996; Claquin *et al.*, 1998; Sokolik and Toon, 1999; Derimian *et al.*, 2008). Though mineral dust aerosol has these important direct effects on radiative balance, the focus on dust events has been primarily during cloudless periods. It is also important to understand how dust can impact the precipitation at mountain sites, by altering the properties of clouds and precipitation.

Mineral dust aerosols have been observed to act as ice nuclei (IN), though this varies with the size, morphology, crystal structure, and composition of the mineral dust (DeMott *et al.*, 2003a, b; Archuleta *et al.*, 2005; Gallavardin *et al.*, 2008). Studies focused specifically on IN ability of dust have found that they can form ice crystals and enhance/induce precipitation in clouds containing supercooled droplets (Bergeron, 1935; DeMott *et al.*, 2003a; Yuter and Houze, 2003; Creamean *et al.*, 2013). Ice crystal number and size distributions, and therefore snow precipitation, strongly depend on the number and type of IN present. Previous studies have determined that different minerals activate as IN at different temperatures, therefore it is important to determine the mineral dust composition present during these events to understand its potential IN capabilities (Murray *et al.*, 2012). Understanding how mineral dust acts to both create and deplete snow in this region is crucial to understanding the hydrological cycle in these remote regions and assess any changes in a changing climate (Neff *et al.*, 2008; Carslaw *et al.*, 2010).

In this study, atmospheric particles were collected at the Swamp Angel Study Plot (SASP), a remote sampling site in the SBBSA, on April 2nd–4th of 2015 to determine the size, morphology, and composition of mineral dust particles present during a minor dust event. During the study, aerosol particles were collected in the size range of 700 nm–5 μm before, during, and after a minor dust deposition event using a microanalysis particle sampler (MPS). Particles were analyzed using scanning electron microscopy (SEM) with energy dispersive X-ray (EDX) spectroscopy, manually and by using computer-controlled SEM (CCSEM). In addition to this, surface snow samples were collected daily to determine the number concentration and size distribution of insoluble residues (the non-dissolved components of particles taken up into precipitation) using a novel technique, nanoparticle tracking analysis (NTA) (Axson *et al.*, 2014). Previous studies have determined that insoluble residues are important as they can provide valuable information about aerosol-cloud-precipitation interactions and processes that aerosol particles can undergo in the atmosphere (Holecek *et al.*, 2007; Ault *et al.*, 2011; Creamean *et al.*, 2013; Creamean *et al.*, 2014). In combination, the ambient mineral dust aerosol and insoluble snow residues provide information regarding mineral dust deposition and integration within the snowpack.

METHODS

Ambient Aerosol and Surface Snow Sampling

Daily collection of ambient particles and surface snow were conducted at the Center for Snow and Avalanche Studies (CSAS) Swamp Angel Study Plot (37.906914 N, –107.711322 W; 11,060') located in the San Juan Mountains of Colorado (Fig. 1(a)). Aerosol particle samples were collected continuously from 11:00 April 2nd to 16:10 April 4th using a three stage microanalysis particle sampler (MPS; California Measurements, Inc.). The MPS collected particles with three size cuts leading to the following ranges: 2.5–5 μm (stage 1), 700 nm–2.5 μm (stage 2), and < 700 nm (stage 3). Ambient air was sampled with the MPS at 2 L min^{-1} and was operated via battery pack to avoid any particulate contamination from a combustion-based power

source, such as a generator. For protection from weather, the MPS was enclosed in a metal electrical box (Fig. 1(b)). Aluminum foil substrates were used for stages 1 and 2, and a carbon TEM grid (Ted Pella, Inc.) for stage 3. The filter substrates were changed twice daily on April 2nd, 3rd, and 4th of 2015, once in the morning and once in the evening for separation of daytime and nighttime samples (Table 1).

Surface snow samples were collected at the SASP near the MPS instrument sampling platform using plastic bags. Samples were then transferred into plastic bottles and allowed to thaw and remained at room temperature for 4 days before being transported to Michigan and stored at 4°C prior to and during analysis.

Ambient Aerosol and Insoluble Snow Residue Analysis

Ambient aerosol samples were analyzed at the Electron Microbeam Analysis Laboratory (EMAL) located at the University of Michigan in Ann Arbor using SEM with EDX.

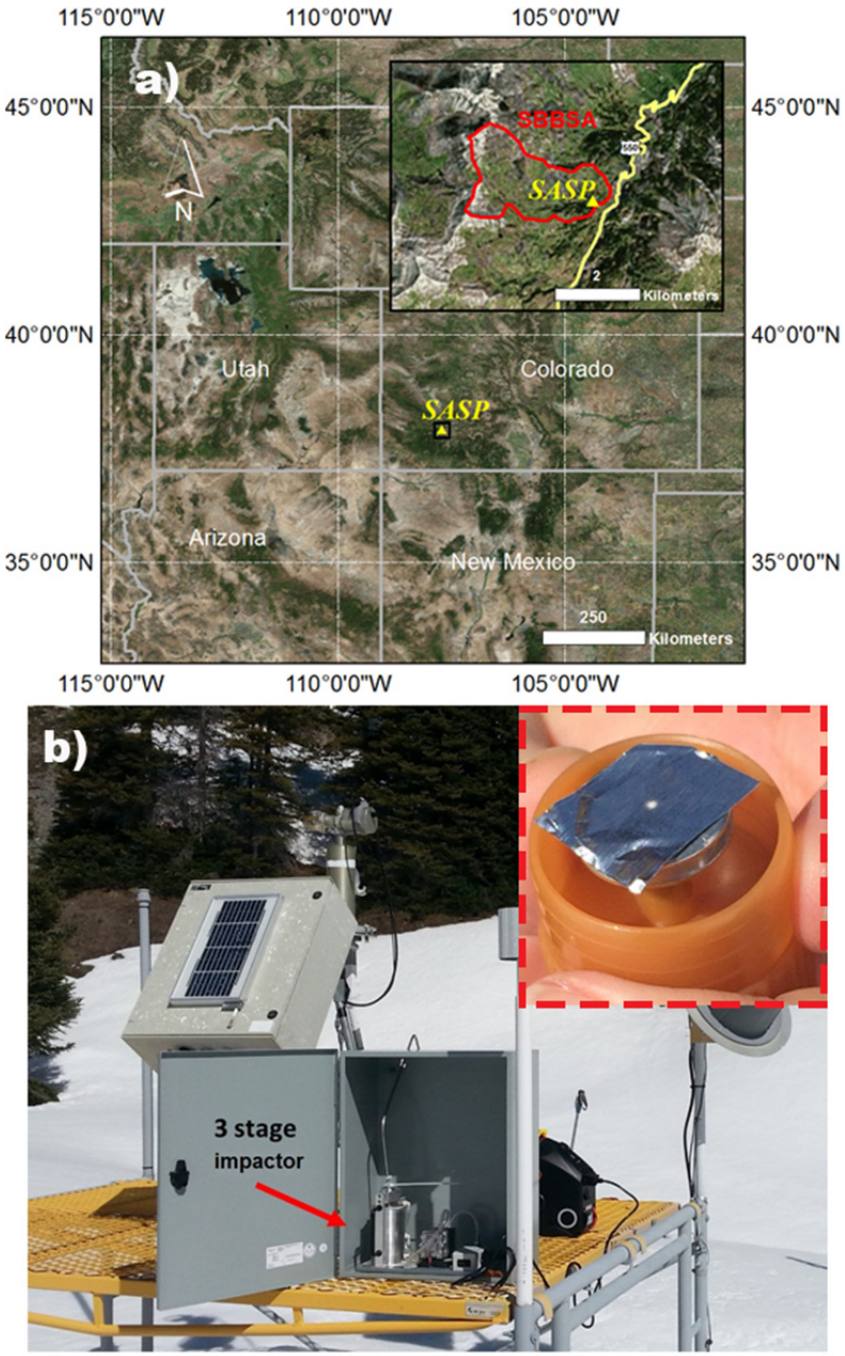

Fig. 1. (a) An image showing the southwestern United States with the inset showing the Swamp Angel Study Plot (red marker) located in the San Juan Mountains, Colorado and (b) image of the MPS on a platform at the sampling site, with the inset showing visible sample loading on aluminum foil substrate on stage two.

Table 1. MPS aerosol particle sampling intervals during Central Mountain Time.

Date	Day Sampling	Night Sampling
4/2/2015	11:00–17:05	17:30–9:40 [a]
4/3/2015	9:40–16:56	17:00–8:45 [a]
4/4/2015	9:00–16:10	

[a] Battery lost charge overnight, though loading suggests sampling occurred through most of the period.

An FEI Nova and FEI Helios both with environmental dual FIB/SEM and Schottky field emitters operating at 15 kV and a secondary electron detector were used to collect secondary electron images and EDX spectra of individual mineral dust particles from stages 1 and 2. It should be noted that as the samples were collected on an aluminum substrate the aluminum peak within the dust particles could not be quantified and was excluded from analysis.

To assess the elemental composition of a population of single particles, computer controlled SEM-EDX (CCSEM-EDX) was employed to analyze a greater quantity of particles. Information from the SEM-EDX allowed us to determine the elements to be used for CCSEM-EDX including, C, N, O, Na, Mg, Si, P, S, Cl, K, Ca, Ti, and Fe. Up to 300 particles per substrate were analyzed for each ambient sample, which allowed statistical analysis. A total of 1,308 particles were analyzed with CCSEM. CCSEM-EDX was performed using EDAX Genesis Software at EMAL. Atomic percentages of elements present from each particle analyzed were integrated into MatLab (Mathworks, Inc.) as a matrix using the procedure described in Ault *et al.* (2012). All samples were then grouped into 10 clusters using the K-means algorithm, which represented the asymptote of diminishing reduction in error with increasing numbers of clusters. The clusters were grouped manually into particle types based on similarity of spectra and ambient particle data in the literature (Song *et al.*, 1999; Falkovich *et al.*, 2001; Krueger *et al.*, 2004; Coz *et al.*, 2009; Ault *et al.*, 2012; Fitzgerald *et al.*, 2015).

The size distribution and total number concentration of insoluble residues in the melted snow samples were determined using nanoparticle tracking analysis (NTA; LM10, Nanosight™), which has been described previously (Filipe *et al.*, 2010; Carr and Wright, 2013; Axson *et al.*, 2014). When considering the NTA data two important caveats should be noted: 1) the upper size limit of the instrument is 1 μm and 2) no chemical information is obtained, so it must be inferred. The samples were collected in the morning each day, so changes during the dust event on the night of April 2nd would be observed in snow collected the following morning on April 3rd. Thus, for completeness, the aerosol and surface snow samples correspond such that the snow sample on April 2nd, April 3rd, and April 4th correspond with aerosol sampling on the afternoon of April 2nd, overnight on April 2nd–3rd, and overnight April 3rd–4th, respectively. Prior to analysis, each sample was shaken to resuspend any settled particles. Videos were captured for each sample with 10 × 60 second videos using a 500-μL aliquot of each precipitation sample loaded into a 1-mL syringe operated by a syringe pump. Sample videos were processed and averaged after each experiment providing the size distribution (particles cm^{-3}) and output in 64 bins per decade.

HYSPLIT Particle Source Analysis

Forty-eight hour back trajectories at the sampling site were calculated hourly during the sampling period starting from 10:00 April 2nd to 16:00 on April 4th using the Hybrid Single Particle Lagrangian Integrated Trajectory (HYSPLIT-4.8, Windows-based version 4) (Draxler and Rolph, 2011). Forty-eight hour trajectories were selected to explain the regional sources and transport pathways (Neff *et al.*, 2008). Trajectories initiated at altitudes of 100, 200, 300, 400, 500, 1000, 2000, 3000, 4000, and 5000 m AGL were calculated to determine trends throughout the lower troposphere. The height of 500 m was selected since trajectories at altitudes of 100, 200, 300, 400, and 500 m showed very similar pathways, likely residing in the boundary layer, while trajectories at higher altitudes quickly transitioned to the free troposphere and would not be representative of the heights at which transport occurred.

RESULTS AND DISCUSSION

Dust Event Characteristics

A minor dust event, with elevated mineral dust content, occurred on April 1st and 2nd in the SBBSA. The Putney Study Plot (3,756 m) of CSAS's Colorado Dust on Snow (CODOS) program is located on the ridgeline above the SASP and provided unobstructed wind data. Dust transport events are frequently observed at SBBSA, where Colorado Plateau dust is deposited (Lawrence *et al.*, 2010). The dust event, which was the first of 2015, was characterized by high winds (10.5 m s^{-1} average, peak gust 30.8 m s^{-1}) from the southwest, which shifted westerly during the event. Details of the back trajectories during the dust transport event are discussed below. Additionally, the event occurred after a dry period with < 1 mm of precipitation from a brief squall. The mass of mineral dust collected in the snowpack for this event was 0.522 g m^{-2} and determined using gravimetric methods as previously described (Goldstein *et al.*, 2008; Painter *et al.*, 2012). This event ranks on the lower end in the range of dust transport events observed by the CODOS project at SASP, for example, during the 2014 season the average loading was 2.58 g m^{-2} from 10 dust events, with a maximum of 7.18 g m^{-2}. Though this was a low intensity event, the presence of mineral dust in the snowpack was observable through subtle changes in the color of the surface snow layer, as were changes in the composition and properties of the particles and snow collected.

Mineral Dust Composition and Size

Single particle analysis is an important method for determining the mineral content present in individual particles. Analysis of iron-containing dust particles has shown that many minerals are commonly present in a single atmospheric particle (Ault *et al.*, 2012). From an atmospheric radiative forcing perspective, the single-particle composition of these dust particles is important. For example, two

hypothetical dust samples each containing ten particles, one sample with one absorbing hematite particle along with nine non-absorbing quartz particles will have very different radiative properties than if all ten particles contained a fraction of absorbing hematite. Hematite and goethite have been identified as the main iron-containing minerals in CODOS dust and are likely the primary absorbing species in the snowpack (Goldstein *et al.*, 2008). The elemental composition and morphology of particles collected on stages 1 and 2 during the minor dust event were initially characterized with SEM-EDX. The major elements observed for these samples were C, O, Na, Mg, Si, S, Cl, K, Ca, Ti, and Fe, all of which were present in previous studies in the Colorado Plateau and San Juan Mountains using bulk inductively coupled plasma mass spectrometry (ICP-MS) (Reynolds *et al.*, 2001; Lawrence *et al.*, 2010). For the > 700 nm particles analyzed, only mineral dust particles were evident in the samples, which is unsurprising considering the scarcity of > 500 nm particle sources in the region. Several types of dust with varying morphologies were observed (Fig. 2). Fig. 2(a) shows a particle containing Fe, Si, C, O, K, and Ca, with the secondary electron image showing the particle to be amorphous and is labeled as an Fe-containing particle. Fig. 2(b) shows a particle that contained a greater amount of Mg relative to the other particles sampled. A Ca-containing particle, which is also enriched in Na is shown in Fig. 2(c). Based on the crystal pattern in the image, this particle likely was aqueous when impacted, indicating it was composed of hygroscopic mineral (though not playa salt, as no Cl was present). A particle enriched in Ca, O, and C is shown in Fig. 2(d) and is likely a nearly pure calcite ($CaCO_3$) particle, which the rounded morphology in the electron image also supports. Lastly, a particle enriched in Si and O is shown in Fig. 2(e), which is likely quartz (SiO_2) or a heavily silicon-based aluminosilicate, which the morphology of the particle in the electron image additionally support the identification of primarily quartz. It is important to note that all five particles shown in Fig. 2 contain a non-negligible iron component, suggesting that many if not all of these particles would have at least a small absorbing component.

To better quantify the changes in dust composition during and after the event, as well as the contribution of particles with enhanced absorption, CCSEM-EDX was used. This provided a sufficient number of particles to apply the K-means clustering algorithm with statistics to provide a meaningful result (Ault *et al.*, 2012). Five main mineral dust particle types identified from the clustering results were Fe-enriched, Mg-enriched, Ca-enriched, calcite, and quartz. Fig. 3 shows an average spectrum for each particle type (left) and a digital color histogram (right). For the Fe-enriched particle type (Fig. 3(a)), 100% of the particles contained Fe > 5% (atomic %) and 46% contained > 20% Fe. These particles are likely highly enriched in nanohematite or goethite and highly absorbing (Sokolik and Toon, 1999; Lafon *et al.*, 2006). Nearly all (96%) of these particles also contained Ti, a transition metal whose minerals are also highly absorbing, though mostly at 2–10 atomic %. The Mg-enriched particles (Fig. 3(b)) contained the least amount of Fe (only 26% of particles), but 65% of these particles had > 20% Mg. For the Ca-enriched particles (Fig. 3(c)) Ca and Mg were both enhanced, though Fe was also in 96% of particles in low amounts (2–15%). The calcite particles (Fig. 3(d)) all contained Ca, C, and O in roughly proportional ratios for $CaCO_3$. Between 75–80% of the calcite particles had small concentrations of Mg, Si, and Fe. Lastly, the quartz particles all had Si and O, with 100% of particles being composed of 30–50% Si and O, as would be expected for quartz. Fe was present in 95% of these particles though in small (2–10%) amounts. Taken together these data show the wide variety of minerals observed during the measuring period, but that nearly all of the particles had some Fe, though the amount and how absorbing the particles are varies greatly by type.

Beyond the types of particles observed, it was also important to know their respective sizes. Normalized particle size distributions for the five mineral dust types are shown in Fig. 4, along with log-normal fits of the size distributions. As these data are number-based and the upper size limit of the MPS impactor was 5 μm, the size distributions were much smaller than the volume-based data (Lawrence *et al.*, 2010) shown in previous analysis of dust in snow samples from the site (which peaked ~50 μm), however when converted to number-based, this would be closer to 1 μm. Of the particle types observed, the Mg-enriched had the smallest mode size (1.5 μm), as did the quartz-type (1.6 μm), both of which had very low amounts of Fe. These two types were likely the smallest contributors to radiative forcing after deposition. The Ca-enriched and calcite were the next largest (1.6 and 1.7 μm modes) and nearly all contained some Fe. Lastly, the largest particles were the Fe-enriched type, which peaked at 2.1 μm, and were likely the greatest contributors to radiative forcing within the snowpack. The relative contributions of these particles to the mineral dust population, as well as their size, will be the determining factor as to the amount of absorption per mass the dust will have after deposition.

Based on the chemical and size properties of each dust type discussed above, changes in the relative amounts of these types present in each sample could be determined during and after the minor dust event on the evening of April 2nd (Fig. 5). Changes in the particle chemical composition were evident after the event for both MPS particle stages sampled. The coarse particles from 2.5–5.0 μm (Fig. 5(a)) were primarily Fe- and Mg-enriched particles during the dust event, with up to 25% Fe-enriched. After the dust event, however, the coarse particles consisted primarily of quartz, calcite, and Ca-enriched dust. This indicates that the ambient particles that were depositing during the dust event were likely more absorbing overall than the particles after the event. Fine particles (0.7–2.5 μm) also showed changes during and after the dust event (Fig. 5(b)), specifically a delayed trend in comparison with the coarse particles. The Mg-enriched and Fe-enriched particles were eventually enhanced, but roughly 12 hours after the coarse particles. The likely explanation for this is the deposition velocity of an ambient mineral dust particle is directly related to its aerodynamic diameter, with a 5 μm particle settling at 25 times greater velocity than a 1 μm particle with the same

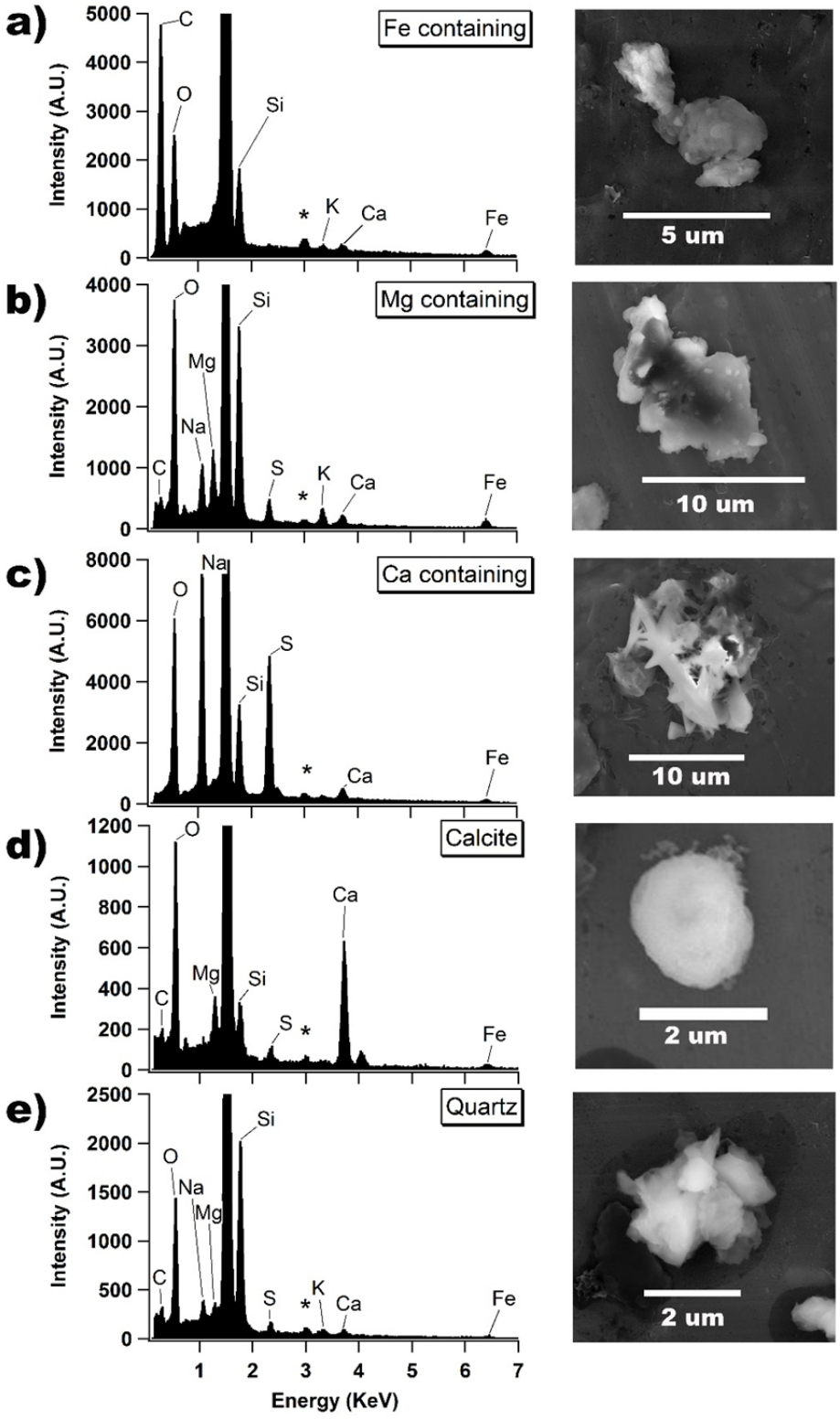

Fig. 2. SEM images and corresponding EDX spectra for the main mineral dust particle types including (a) Fe-enriched, (b) Mg-enriched, (c) Ca-enriched, (d) calcite, and (e) quartz. *Note the signal is primarily from the aluminum substrate.

density (Hinds, 1999). Thus, even though both fine and coarse Fe-enriched and Mg-enriched particles are likely from the same source region, the timing at which they may be incorporated into the snow pack can be different. It is important to note here that an assumption is made that the ambient collected dust is representative of the dust incorporated into the snowpack. This has two important implications: 1) the deposition of absorbing material may extend over a longer time period than a purely mass or volume based sampling method would imply and 2) the

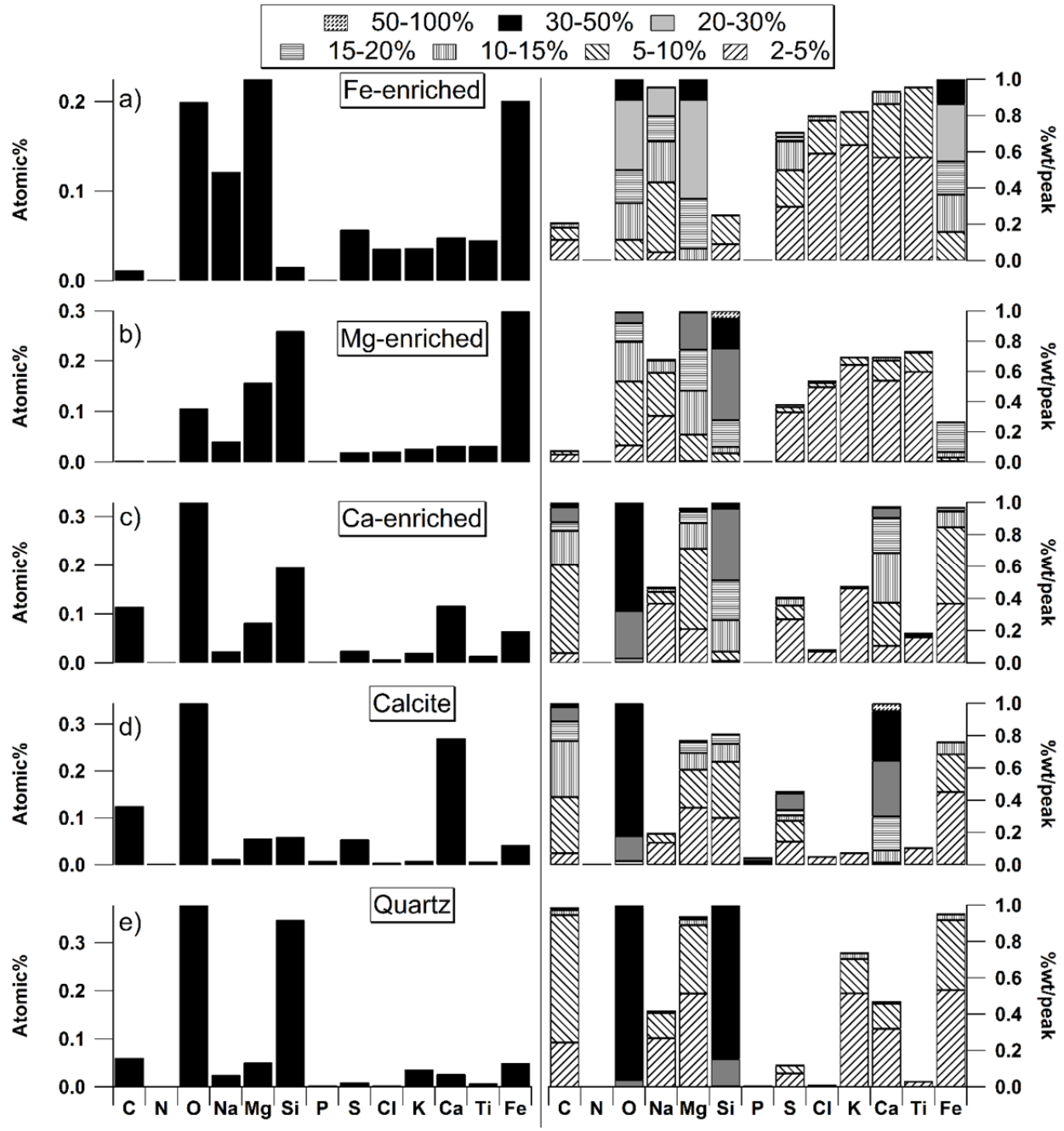

Fig. 3. Average spectra and digital color histograms of different particle classes all containing iron: (a) Fe-enriched dust, (b) Mg-enriched dust, (c) Ca-enriched dust (d) calcite dust, and (e) quartz dust. Average spectra are shown as relative X-ray peak areas across the 13 elements analyzed by CCSEM-EDX (C, N, O, Na, Mg, Si, P, S, Cl, K, Ca, Ti, and Fe). Digital color histogram heights represent the fraction of particles containing a specific element, and colors represent the fraction containing specific ranges of intensities. Note that Al was not used given that the substrate was aluminum foil which does not exclude its presence in these particles.

Mg-enriched and Fe-enriched particles are likely from the same source region. This indicates that the dust events bring in elevated amounts of absorbing dust in comparison to local dust sources, which will have larger impacts on the melting of the snow pack. It is important to connect these shifts in composition at different sizes for the ambient mineral dust particles to the properties of the mineral dust after it is incorporated into the snowpack, both for validation of the ambient trends and to decipher contributions and impacts of different types.

Insoluble Snow Residue Size Distributions and Total Particle Concentrations

The number concentration and size distribution of insoluble residues in the melted surface snow provide a new perspective on quantifying the contribution of dust within

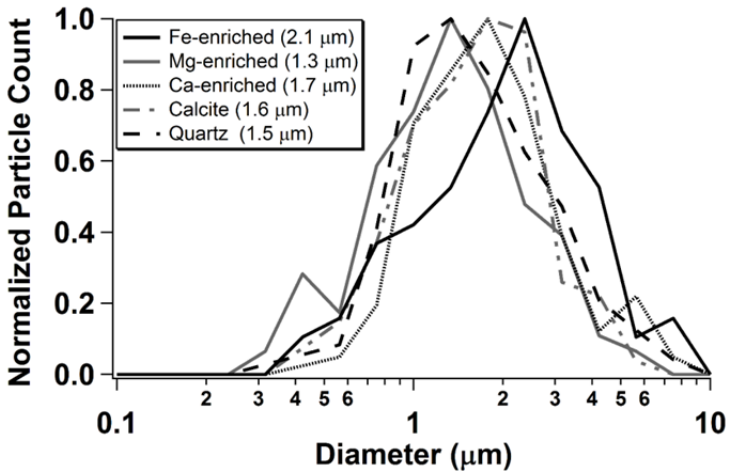

Fig. 4. Normalized particle size distributions for each of the five mineral dust particle types identified combining Stage 1 (2.5–5 μm) and Stage 2 (700 nm–2.5 μm) including their peak mode diameters.

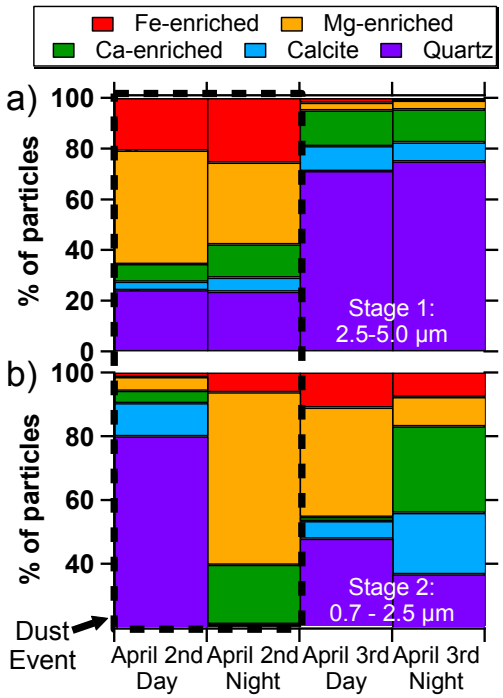

Fig. 5. Relative contributions of different types of mineral dust during day and night samples on April 2nd and 3rd with the MPS (a) Stage 1 (2.5–5 μm) and (b) Stage 2 (700 nm–2.5 μm).

snow, which was measured for the first time with NTA in 2014 for both precipitated rain and snow (Axson *et al.*, 2014). Based on the composition of the particles on Stages 1 and 2, as well as Stage 3 (not shown), it is very likely that the largest contributor to the number concentration, particularly at > 0.1 μm, is mineral dust. Figs. 6(a) and 6(b) show the raw and log-normally fitted insoluble residue size distributions from melted snow samples collected daily at the SASP on April 2nd, 3rd, and 4th. The insoluble residues in the melted snow from the beginning of the dust event shows a peak in the distribution at 203 nm, while the mode after the event is 197 nm (Fig. 6(b)). Snow collected from the dust event showed a significant shift to larger particles sizes, with a mode at 221 nm, well beyond the uncertainty

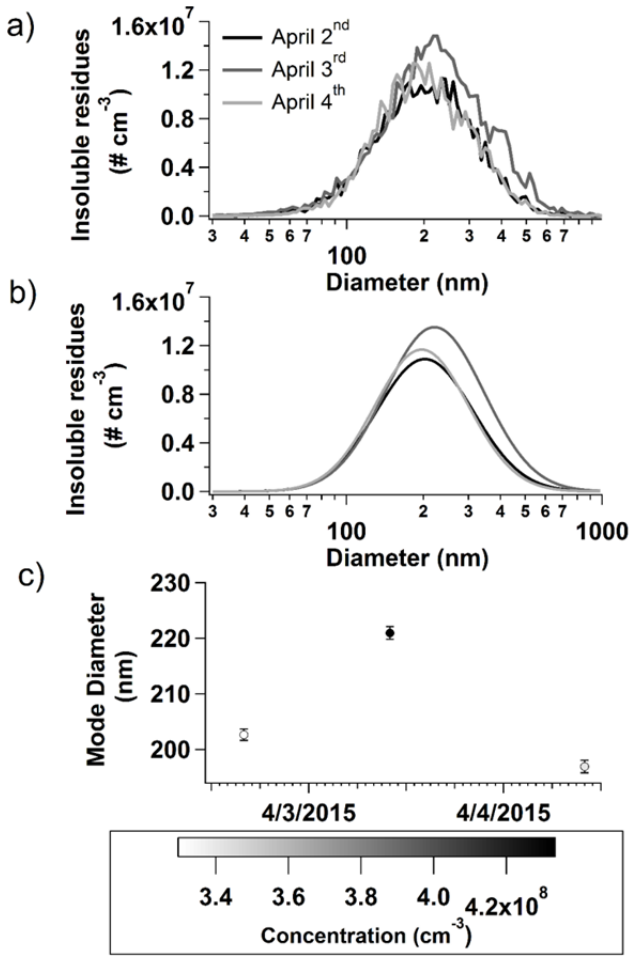

Fig. 6. (a) NTA raw size distributions for the three surface snow sampling days and (b) the log-normally fit size distributions. (c) A plot showing the variation in size and total concentration for three sampling periods.

of the measurement (Fig. 6(b)). The number concentration for the dust event was also 21–24% greater than the number concentrations on April 2nd and April 4th (Fig. 6(c)). These results align well with the ambient data, indicating larger Fe-enriched dust particles were deposited on the snow surface during the dust event, which are more absorbing.

As the samples were transported back to Michigan in a melted form it was important to establish that the mode and number concentrations did not change quickly under the transport and storage conditions. Changes in insoluble residues during storage were evaluated weekly for three weeks after the samples were collected and transported from Colorado to Michigan (Fig. 7). The April 2nd sample had a shift in the mode within the uncertainty of the instrument from Week 1 to 2 after collection, with an increase observed in Week 3 after collection. The insoluble residue size distribution and number concentration from April 3rd had little change due to storage over all 3 weeks. The melted snow samples from April 4th appear to be stable for the first two weeks of storage, similar to April 2nd. These changes in size during the third week of storage may be due to coagulation of insoluble residues, settling of residues, or adhesion to the walls of the storage containers. Therefore, based on results it is believed that the melted snow samples will be stable for up to two weeks after collection and storage in plastic bottles and that the storage time could be extended with more complicated preparation and storage methods.

Mineral Dust Source Analysis

For dust transport to occur to the San Juan Mountains, three conditions must be met: 1) low soil moisture and/or soil disturbance in the source regions leading to loose soil surfaces, 2) high wind speeds for soil disturbance, and 3) wind directions leading to the San Juan Mountains (Lawrence *et al.*, 2010). Though soil moisture was higher through most of March 2015, by the beginning of April soil moisture in the Colorado Plateau ranged from 10–20 kg m^{-2} which was low enough for dust transport to occur (Acker and Leptoukh, 2007). As noted above, wind direction and wind speed from the ridgeline above the SASP (at Putney) averaged 10.8 m s^{-1} from the southwest and west during the event. HYSPLIT 48-hour back trajectories were used to gain expanded insight regarding the source regions and transport pathways of the mineral dust being deposited at the SASP (Fig. 8). Another important parameter for dust transport is that the air masses reaching the San Juan Mountains need to be close enough to the surface of the dust source regions for mineral dust to be entrained by the high winds. During the dust event in the daytime on April 2nd, the air mass back trajectories passed over the northeast Arizona portion of the Colorado Plateau southwest of the SASP. The heights of these trajectories maintained contact with the surface over the full 48 hours during the day on April 2nd, indicating that dust could be picked up from the surface and transported. Overnight on April 2nd into the 3rd

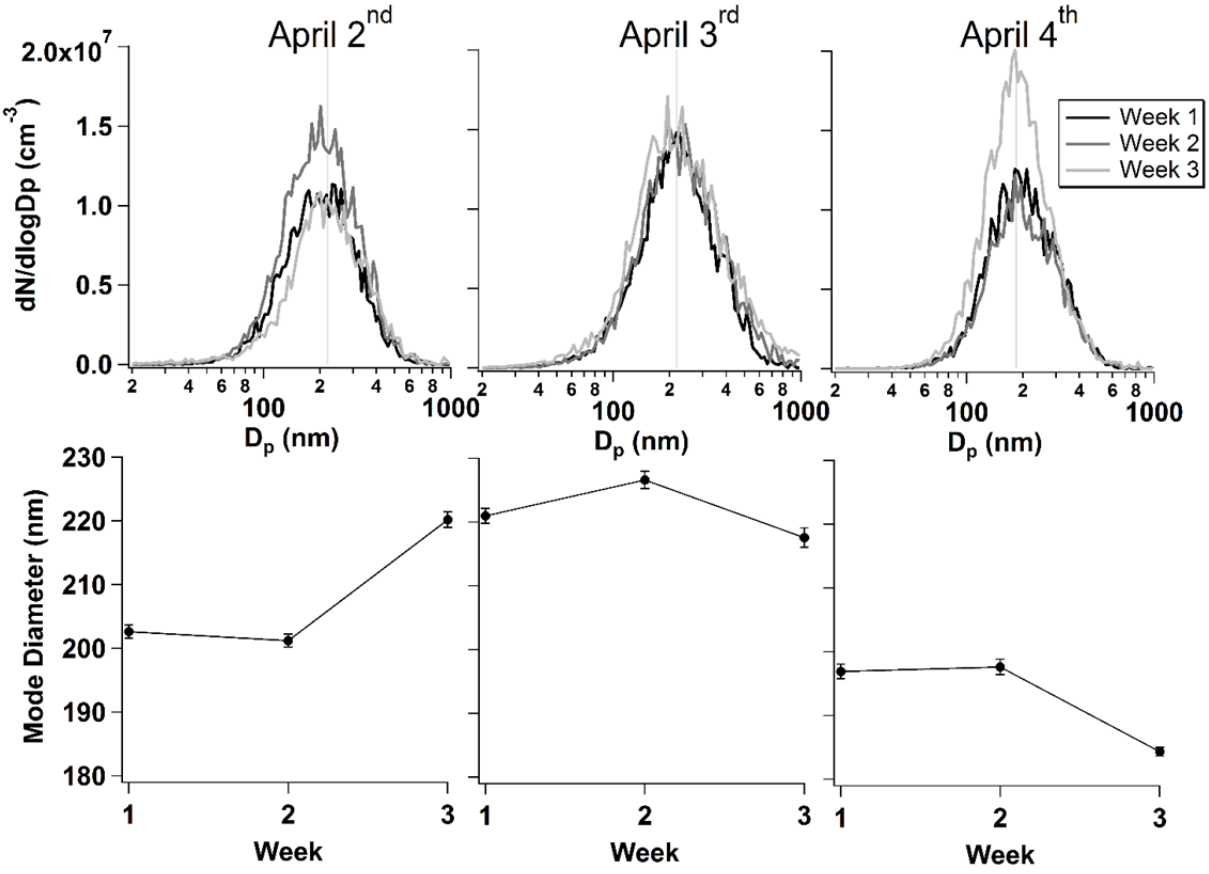

Fig. 7. Analysis of storage for insoluble residues of melted snow stored for up to 3 weeks after collection in plastic water bottles and analyzed using NTA.

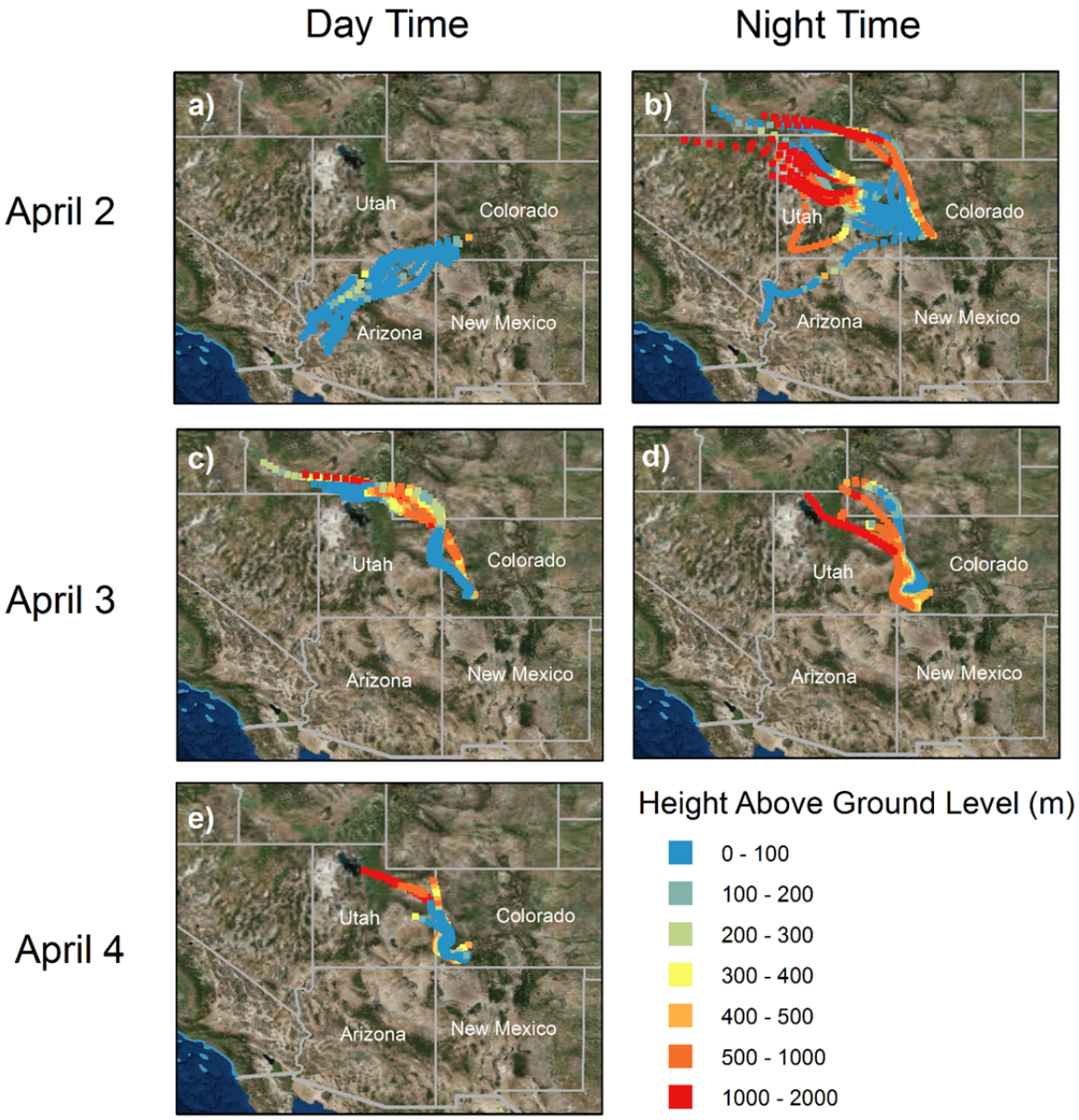

Fig. 8. Hourly back trajectories initiated at an altitude 500 m above ground level are shown for all sampling periods, (a) April 2nd daytime, (b) April 2nd nighttime, (c) April 3rd daytime, (d) April 3rd nighttime, and (e) April 4th daytime samples, with the colors representing the various height ranges.

the air masses shifted from the southwest to the northwest passing over southeast and eastern Utah with trajectories flowing near the surface for 24–30 hours before reaching elevations above the boundary layer from 30–48 hours. This is consistent with the microscopy data showing that the dust event was primarily on April 2nd with less flow near the surface on April 3rd such that there is less dust transport. By the morning of April 3rd the flow was consistently approaching the SASP from the northwest passing over northeastern Utah and southwestern Wyoming. For the remaining sampling time periods (April 3 daytime, April 3 nighttime, and April 4 daytime), the air masses continued to come from the northwest through northeastern Utah. Later on April 3rd and parts of April 4th, the flow was less consistent, but frequently elevated above the boundary layer within a few hours from the SASP, indicating that flow conditions were more unfavorable for dust transport than previously used for the San Juan Mountain region (Neff *et al.*, 2013). Taken together the source analysis corroborates with our microscopy data indicating changes in ambient and snowpack mineral dust during and after the dust event on April 2nd. This is also in agreeance with prior studies of dust in snow from CODOS, which the results herein connect with the composition in ambient particles prior to deposition.

CONCLUSIONS

The results herein connecting ambient aerosol composition and mineralogy with the number concentration and size

distributions of insoluble residues at the surface of snow represent an important initial step at linking the atmosphere and cryosphere. It was determined that during dust events at the SASP of the SBBSA there was an influx of Fe-enriched dust, which leads to greater number concentrations and larger dust particles in the snow pack. This dust had greater absorption potential and likely had a larger climate footprint than quartz observed in the coarse particles after the event. Though there was no indication of contributions from black carbon, we cannot definitively rule out a small contribution to the radiative forcing given that specific measurements were not made for black carbon. The shift in dust composition and insoluble residue size and concentrations was corroborated by HYSPLIT back trajectory analysis and the shift in source region and wind speed as the event ended. It was also found that these snow melt samples were stable when stored for up to two weeks at 4°C. This approach for collection, analysis, and storage of mineral dust aerosol and insoluble snow melt residues has the potential to be applied to other studies in the San Juan and other mountain sites.

A number of aspects of dust-climate interactions were not able to be explored that could provide greater insight into the impact of transported dust on high elevation sites, such as those in the SBBSA. Of particular interest is the impact of dust transport during events with clouds and precipitation. It is not uncommon for transported dust from the Colorado Plateau (or beyond) to be incorporated into the snowpack during periods with precipitation from orographic lifting along the western slope, but to date no studies have attempted to deconvolve the relative importance of dry and wet deposition during those events. This introduces a number of processes and questions that are worthy of future study: 1) Do more intense events have a link between ambient particles and residues in snow (as this event was considered minor at SASP), 2) How do wet versus dry deposited dust interact with solar radiation within the snow pack (i.e., is one more concentrated at the surface), 3) Are certain types of mineral dust preferentially wet scavenged versus dry deposited and 4) Does the transported dust act as IN within the orographic clouds and modify precipitation processes? As dust events increase in a changing and more arid climate within the southwestern United States future efforts are needed to improve our fundamental understanding of the interplay between transported dust, radiative processes, snow melt, hydrology, clouds and precipitation.

ACKNOWLEDGMENTS

Funding for this work was provided by the Michigan Space Grant Consortium. Dr. Harland Goldstein of the United States Geological survey is thanked for providing mass per unit area dust concentrations for the dust event. The Electron Microbeam Analysis Laboratory (EMAL) at the University of Michigan is acknowledged for assistance with electron microscopy. The authors gratefully acknowledge the NOAA Air Resources Laboratory (ARL) for the provision of the HYSPLIT transport and dispersion model and/or READY website (http://www.ready.noaa.gov) used in this publication. Analyses and soil moisture data used in this paper were produced with the Giovanni online data system, developed and maintained by the NASA GES DISC.

REFERENCES

Acker, J.G. and Leptoukh, G. (2007). Online Analysis Enhances Use of Nasa Earth Science Data. *Eos Trans. AGU* 88: 14–17.

Andreae, M.O. and Rosenfeld, D. (2008). Aerosol-Cloud-Precipitation Interactions. Part 1. The Nature and Sources of Cloud-Active Aerosols. *Earth Sci. Rev.* 89: 13–41.

Archuleta, C.M., DeMott, P.J. and Kreidenweis, S.M. (2005). Ice Nucleation by Surrogates for Atmospheric Mineral Dust and Mineral Dust/Sulfate Particles at Cirrus Temperatures. *Atmos. Chem. Phys.* 5: 2617–2634.

Ault, A.P., Williams, C.R., White, A.B., Neiman, P.J., Creamean, J.M., Gaston, C.J., Ralph, F.M. and Prather, K.A. (2011). Detection of Asian Dust in California Orographic Precipitation. *J. Geophys. Res.* 116: D16205.

Ault, A.P., Peters, T.M., Sawvel, E.J., Casuccio, G.S., Willis, R.D., Norris, G.A. and Grassian, V.H. (2012). Single-Particle SEM-EDX Analysis of Iron-Containing Coarse Particulate Matter in an Urban Environment: Sources and Distribution of Iron within Cleveland, Ohio. *Environ. Sci. Technol.* 46: 4331–4339.

Axson, J.L., Creamean, J.M., Bondy, A.L., Capracotta, S.S., Warner, K.Y. and Ault, A.P. (2014). An in Situ Method for Sizing Insoluble Residues in Precipitation and Other Aqueous Samples. *Aerosol Sci. Technol.* 49: 24–34.

Baustian, K.J., Cziczo, D.J., Wise, M.E., Pratt, K.A., Kulkarni, G., Hallar, A.G. and Tolbert, M.A. (2012). Importance of Aerosol Composition, Mixing State, and Morphology for Heterogeneous Ice Nucleation: A Combined Field and Laboratory Approach. *J. Geophys. Res.* 117: D06217.

Bergeron, T. (1935). On the Physics of Cloud and Precipitation, In *5th Assembly of the U.G.G.I.*, Paul Dupont, Paris, pp. 156–178.

Bond, T.C., Doherty, S.J., Fahey, D.W., Forster, P.M., Berntsen, T., DeAngelo, B.J., Flanner, M.G., Ghan, S., Karcher, B., Koch, D., Kinne, S., Kondo, Y., Quinn, P.K., Sarofim, M.C., Schultz, M.G., Schulz, M., Venkataraman, C., Zhang, H., Zhang, S., Bellouin, N., Guttikunda, S.K., Hopke, P.K., Jacobson, M.Z., Kaiser, J.W., Klimont, Z., Lohmann, U., Schwarz, J.P., Shindell, D., Storelvmo, T., Warren, S.G. and Zender, C.S. (2013). Bounding the Role of Black Carbon in the Climate System: A Scientific Assessment. *J. Geophys. Res.* 118: 5380–5552.

Carr, B. and Wright, M. (2013). *Nanoparticle Tracking Analysis: A Review of Applications and Usage 2010-2012*. NanoSight Ltd, Minton Park, London Road, Amesbury, Wiltshire, SP4 7RT.

Carslaw, K.S., Boucher, O., Spracklen, D.V., Mann, G.W., Rae, J.G.L., Woodward, S. and Kulmala, M. (2010). A Review of Natural Aerosol Interactions and Feedbacks within the Earth System. *Atmos. Chem. Phys.* 10: 1701–

1737.
Claquin, T., Schulz, M., Balkanski, Y. and Boucher, O. (1998). Uncertainties in Assessing Radiative Forcing by Mineral Dust. *Tellus Ser. B* 50: 491–505.
Conway, H., Gades, A. and Raymond, C.F. (1996). Albedo of Dirty Snow during Conditions of Melt. *Water Resour. Res.* 32: 1713–1718.
Coz, E., Gomez-Moreno, F.J., Pujadas, M., Casuccio, G.S., Lersch, T.L. and Artinano, B. (2009). Individual Particle Characteristics of North African Dust under Different Long-Range Transport Scenarios. *Atmos. Environ.* 43: 1850–1863.
Creamean, J.M., Lee, C., Hill, T.C., Ault, A.P., DeMott, P.J., White, A.B., Ralph, F.M. and Prather, K.A. (2014). Chemical Properties of Insoluble Precipitation Residues. *J. Aerosol. Sci.* 76: 13–27.
Creamean, J.M., Suski, K.J., Rosenfeld, D., Cazorla, A., DeMott, P.J., Sullivan, R.C., White, A.B., Ralph, F.M., Minnis, P., Comstock, J.M., Tomlinson, J.M. and Prather, K.A. (2013). Dust and Biological Aerosols from the Sahara and Asia Influence Precipitation in the Western U.S. *Science* 339: 1572–1578.
Deems, J.S., Painter, T.H., Barsugli, J.J., Belnap, J. and Udall, B. (2013). Combined Impacts of Current and Future Dust Deposition and Regional Warming on Colorado River Basin Snow Dynamics and Hydrology. *Hydrol. Earth Syst. Sci.* 17: 4401–4413.
DeMott, P.J., Cziczo, D.J., Prenni, A.J., Murphy, D.M., Kreidenweis, S.M., Thomson, D.S., Borys, R. and Rogers, D.C. (2003a). Measurements of the Concentration and Composition of Nuclei for Cirrus Formation. *Proc. Natl. Acad. Sci. U.S.A.* 100: 14655–14660.
DeMott, P.J., Sassen, K., Poellot, M.R., Baumgardner, D., Rogers, D.C., Brooks, S.D., Prenni, A.J. and Kreidenweis, S.M. (2003b). African Dust Aerosols as Atmospheric Ice Nuclei. *Geophys. Res. Lett.* 30: 1–4.
Derimian, Y., Karnieli, A., Kaufman, Y.J., Andreae, M.O., Andreae, T.W., Dubovik, O., Maenhaut, W. and Koren, I. (2008). The Role of Iron and Black Carbon in Aerosol Light Absorption. *Atmos. Chem. Phys.* 8: 3623–3637.
Di Biagio, C., Boucher, H., Caquineau, S., Chevaillier, S., Cuesta, J. and Formenti, P. (2014). Variability of the Infrared Complex Refractive Index of African Mineral Dust: Experimental Estimation and Implications for Radiative Transfer and Satellite Remote Sensing. *Atmos. Chem. Phys.* 14: 11093–11116.
HYSPLIT (HYbrid Single-Particle Lagrangian Integrated Trajectory) Model access via NOAA ARL READY Website, http://ready.arl.noaa.gov/HYSPLIT.php, 2011.
Falkovich, A.H., Ganor, E., Levin, Z., Formenti, P. and Rudich, Y. (2001). Chemical and Mineralogical Analysis of Individual Mineral Dust Particles. *J. Geophys. Res.* 106: 18029–18036.
Filipe, V., Hawe, A. and Jiskoot, W. (2010). Critical Evaluation of Nanoparticle Tracking Analysis (Nta) by Nanosight for the Measurement of Nanoparticles and Protein Aggregates. *Pharm. Res.* 27: 796–810.
Fitzgerald, E., Ault, A.P., Zauscher, M., Mayol-Bracero, O.L. and Prather, K.A. (2015). Comparison of the Mixing State of Long-Range Transported Asian and African Mineral Dust. *Atmos. Environ.* 115: 19–25.
Gallavardin, S.J., Froyd, K.D., Lohmann, U., Moehler, O., Murphy, D.M. and Cziczo, D.J. (2008). Single Particle Laser Mass Spectrometry Applied to Differential Ice Nucleation Experiments at the Aida Chamber. *Aerosol Sci. Technol.* 42: 773–791.
Goldstein, H.L., Reynolds, R.L., Reheis, M.C., Yount, J.C. and Neff, J.C. (2008). Compositional Trends in Aeolian Dust Along a Transect across the Southwestern United States. *J. Geophys. Res. -Earth* 113: 1–15.
Hinds, W.C. (1999). *Aerosol Technology: Properties, Behavior, and Measurements of Airborne Particles*, Wiley, New York.
Holecek, J.C., Spencer, M.T. and Prather, K.A. (2007). Analysis of Rainwater Samples: Comparison of Single Particle Residues with Ambient Particle Chemistry from the Northeast Pacific and Indian Oceans. *J. Geophys. Res.* 112: 1–10.
Hudson, P.K., Gibson, E.R., Young, M.A., Kleiber, P.D. and Grassian, V.H. (2008a). Coupled Infrared Extinction and Size Distribution Measurements for Several Clay Components of Mineral Dust Aerosol. *J. Geophys. Res.* 113: 1–11.
Hudson, P.K., Young, M.A., Kleiber, P.D. and Grassian, V.H. (2008b). Coupled Infrared Extinction Spectra and Size Distribution Measurements for Several Non-clay Components of Mineral Dust Aerosol (Quartz, Calcite, and Dolomite). *Atmos. Environ.* 42: 5991–5999.
Jung, H.J., Eom, H.J., Kang, H.W., Moreau, M., Sobanska, S. and Ro, C.U. (2014). Combined Use of Quantitative Ed-Epma, Raman Microspectrometry, and ATR-FTIR Imaging Techniques for the Analysis of Individual Particles. *Analyst* 139: 3949–3960.
Kleiber, P.D., Grassian, V.H., Young, M.A. and Hudson, P.K. (2009). T-matrix Studies of Aerosol Particle Shape Effects on IR Resonance Spectral Line Profiles and Comparison with an Experiment. *J. Geophys. Res.* 114: 1–10.
Klueser, L., Kleiber, P., Holzer-Popp, T. and Grassian, V.H. (2012). Desert Dust Observation from Space - Application of Measured Mineral Component Infrared Extinction Spectra. *Atmos. Environ.* 54: 419–427.
Krueger, B.J., Grassian, V.H., Cowin, J.P. and Laskin, A. (2004). Heterogeneous Chemistry of Individual Mineral Dust Particles from Different Dust Source Regions: The Importance of Particle Mineralogy. *Atmos. Environ.* 38: 6253–6261.
Lafon, S., Sokolik, I.N., Rajot, J.L., Caquineau, S. and Gaudichet, A. (2006). Characterization of Iron Oxides in Mineral Dust Aerosols: Implications for Light Absorption. *J. Geophys. Res.* 111: 1–19.
Laskina, O., Young, M.A., Kleiber, P.D. and Grassian, V.H. (2012). Infrared Extinction Spectra of Mineral Dust Aerosol: Single Components and Complex Mixtures. *J. Geophys. Res.* 117: 1–10.
Lau, W.K.M., Kim, M.K., Kim, K.M. and Lee, W.S. (2010). Enhanced Surface Warming and Accelerated Snow Melt in the Himalayas and Tibetan Plateau Induced

by Absorbing Aerosols. *Environ. Res. Lett.* 5: 1–10.

Lawrence, C.R., Painter, T.H., Landry, C.C. and Neff, J.C. (2010). Contemporary Geochemical Composition and Flux of Aeolian Dust to the San Juan Mountains, Colorado, United States. *J. Geophys. Res.* 115: 1–15.

Murray, B.J., O'Sullivan, D., Atkinson, J.D. and Webb, M.E. (2012). Ice Nucleation by Particles Immersed in Supercooled Cloud Droplets. *Chem. Soc. Rev.* 41: 6519–6554.

Neff, J.C., Ballantyne, A.P., Farmer, G.L., Mahowald, N.M., Conroy, J.L., Landry, C.C., Overpeck, J.T., Painter, T.H., Lawrence, C.R. and Reynolds, R.L. (2008). Increasing Eolian Dust Deposition in the Western United States Linked to Human Activity. *Nat. Geosci.* 1: 189–195.

Neff, J.C., Reynolds, R.L., Munson, S.M., Fernandez, D. and Belnap, J. (2013). The Role of Dust Storms in Total Atmospheric Particle Concentrations at Two Sites in the Western Us. *J. Geophys. Res.* 118: 11201–11212.

Painter, T.H., Barrett, A.P., Landry, C.C., Neff, J.C., Cassidy, M.P., Lawrence, C.R., McBride, K.E. and Farmer, G.L. (2007). Impact of Disturbed Desert Soils on Duration of Mountain Snow Cover. *Geophys. Res. Lett.* 34: 1–6.

Painter, T.H., Skiles, S.M., Deems, J.S., Bryant, A.C. and Landry, C.C. (2012). Dust Radiative Forcing in Snow of the Upper Colorado River Basin: 1. A 6 Year Record of Energy Balance, Radiation, and Dust Concentrations. *Water Resour. Res.* 48: 1–14.

Reynolds, R., Belnap, J., Reheis, M., Lamothe, P. and Luiszer, F. (2001). Aeolian Dust in Colorado Plateau Soils: Nutrient Inputs and Recent Change in Source. *Proc. Natl. Acad. Sci. U.S.A.* 98: 7123–7127.

Skiles, S.M., Painter, T.H., Deems, J.S., Bryant, A.C. and Landry, C.C. (2012). Dust Radiative Forcing in Snow of the Upper Colorado River Basin: 2. Interannual Variability in Radiative Forcing and Snowmelt Rates. *Water Resour. Res.* 48: 1–11.

Sobanska, S., Hwang, H., Choel, M., Jung, H.J., Eom, H.J., Kim, H., Barbillat, J. and Ro, C.U. (2012). Investigation of the Chemical Mixing State of Individual Asian Dust Particles by the Combined Use of Electron Probe X-Ray Microanalysis and Raman Microspectrometry. *Anal. Chem.* 84: 3145–3154.

Sobanska, S., Falgayrac, G., Rimetz-Planchon, J., Perdrix, E., Bremard, C. and Barbillat, J. (2014). Resolving the Internal Structure of Individual Atmospheric Aerosol Particle by the Combination of Atomic Force Microscopy, Esem-Edx, Raman and Tof-Sims Imaging. *Microchem. J.* 114: 89–98.

Sokolik, I.N. and Toon, O.B. (1996). Direct Radiative Forcing by Anthropogenic Airborne Mineral Aerosols. *Nature* 381: 681–683.

Sokolik, I.N. and Toon, O.B. (1999). Incorporation of Mineralogical Composition into Models of the Radiative Properties of Mineral Aerosol from UV to IR Wavelengths. *J. Geophys. Res.* 104: 9423–9444.

Song, X.H., Hadjiiski, L., Hopke, P.K., Ashbaugh, L.L., Carvacho, O., Casuccio, G.S. and Schlaegle, S. (1999). Source Apportionment of Soil Samples by the Combination of Two Neural Networks Based on Computer-Controlled Scanning Electron Microscopy. *J. Air Waste Manage. Assoc.* 49: 773–783.

Warren, S.G. and Wiscombe, W.J. (1980). A Model for the Spectral Albedo of Snow 2. Snow Containing Atmospheric Aerosols. *J Atmos Sci* 37: 2734–2745.

Yuter, S.E. and Houze, R.A. (2003). Microphysical Modes of Precipitation Growth Determined by S-Band Vertically Pointing Radar in Orographic Precipitation during Map. *Q. J. R. Meteorolog. Soc.* 129: 455–476.

Received for review, May 16, 2015
Revised, August 2, 2015
Accepted, September 8, 2015